Tectonics

RESEARCH ARTICLE
10.1029/2020TC006383

Key Points:
- The classic Catalina core complex main mylonitic fabric did not form synchronous with the brittle detachment fault but much earlier
- Ductile fabric is developed during the Eocene and is constrained by age of late kinematic dikes
- The entire section was located shallow beneath the surface (some 5 km) at the time of brittle Basin and Range detachment faulting (25 Ma)

Supporting Information:
- Supporting Information S1
- Data S1
- Data S2
- Data S3
- Figure S1

Correspondence to:
M. N. Ducea,
ducea@arizona.edu

Citation:
Ducea, M. N., Triantafyllou, A., & Krcmaric, J. (2020). New timing and depth constraints for the Catalina Metamorphic Core complex, Southeast Arizona. *Tectonics*, *39*, e2020TC006383. https://doi.org/10.1029/2020TC006383

Received 17 JUN 2020
Accepted 3 AUG 2020
Accepted article online 15 AUG 2020

New Timing and Depth Constraints for the Catalina Metamorphic Core Complex, Southeast Arizona

Mihai N. Ducea[1,2], Antoine Triantafyllou[1,4], and Jordan Krcmaric[1,3]

[1]Department of Geosciences, University of Arizona, Tucson, AZ, USA, [2]Faculty of Geology and Geophysics, University of Bucharest, Bucharest, Romania, [3]National Geodetic Survey, National Oceanic and Atmospheric Administration (NOAA), Silver Spring, MD, USA, [4]Departement of Geologie, Université of Liège, Liège, Belgium

Abstract The Santa Catalina-Tortolita-Rincon Mountains of Southeast Arizona are a classic metamorphic core complex (MCC) and represent footwall exposures of crustal rocks exhumed by a detachment system. This study presents new evidence for the formation of the majority of ductile deformation during the Eocene (~46 Ma), synchronous with the emplacement of the regionally significant Wilderness Sills Suite (57–45 Ma). The evidence is provided by Eocene U-Pb ages of syn- to late kinematic dikes emplaced in the principal ductile mylonitic fabric of the Catalina forerange, earlier than the brittle normal fault system and the formation of Tucson basin beginning with the latest Oligocene. Well-documented shear sense indicators may not reflect extension at that time (Eocene), but more likely the direction of crustal flow now rotated during later extension. Muscovite-plagioclase Rb-Sr isochron ages of three mylonitic rocks are all clustered around 34 Ma, which is inferred to be the last age when these rocks were being deformed under ductile conditions following the emplacement of the Wilderness Sills Suite and various related dikes. Biotite-plagioclase Rb-Sr ages on the same rocks demonstrate that the section cooled below ~300°C at 25–26 Ma during the development of normal faulting. Normal faulting was synchronous with the emplacement of the Catalina Intrusive Suite. New U-Pb age results for Catalina Intrusive Suite indicate a combined mean age of 24.9 Ma. Chemical compositions of hornblende-plagioclase pairs were obtained on six Catalina Intrusive Suite samples; depth estimates for the emplacement of the Catalina Intrusive Suite average of about 6 km. These results suggest that the exposed Catalina ductile detachment system was at about 5 km beneath the surface at 25 Ma. These new data bring new light into the development of this core complex and suggest that the similarity in orientations of *principal* ductile and brittle fabrics at the Catalina MCC locality are coincidental. Neither was the principal ductile fabric developed during the low-angle normal faulting of the latest Oligocene nor was this exposed section a midcrustal one at that time. Transient, pluton emplacement-enhanced, and extension-related ductile deformation at shallow crustal levels operated locally at ~25 Ma but that does not account for the development of the majority of the Catalina MCC mylonites.

1. Introduction

The Santa Catalina, Tortolita, and Rincon Mountains of southeast Arizona are structurally a well-established late Oligocene metamorphic core complex (MCC) in the southwestern United States Basin and Range province, comprising a mylonite zone exposed immediately below a low-angle detachment system, the Catalina detachment fault (Crittenden et al., 1978; Davis & Coney, 1979; Dickinson, 1991; Keith et al., 1980; Figure 1a). Referred simply to as the *Catalina MCC*, it is typical of parts of the highly extended Basin and Range province (Wernicke, 1985). Several MCCs are well-documented in southeast California and southern Arizona (Singleton et al., 2019, and references therein), and their development is believed to coincide with a change in the tectonic regime of western North America from compressional to extensional in the middle Cenozoic, leading to a collapse of overthickened crust (Chapman et al., 2015; Coney & Harms, 1984), possibly of an orogenic plateau (Chapman et al., 2020). The unroofing of these plastically deformed crustal units beneath brittle detachment fault systems has traditionally been interpreted as representing high magnitude low-angle fault systems that cut into the brittle-ductile transition (Lister & Davis, 1989; Spencer & Reynolds, 1989; Wernicke, 1992). Consequently, the exposures seen in the footwall of detachment systems represent exhumed midcrustal fragments. Originally discovered in the American Southwest and the Pacific Northwest of the North American Cordillera (Davis, 1980, for an early history

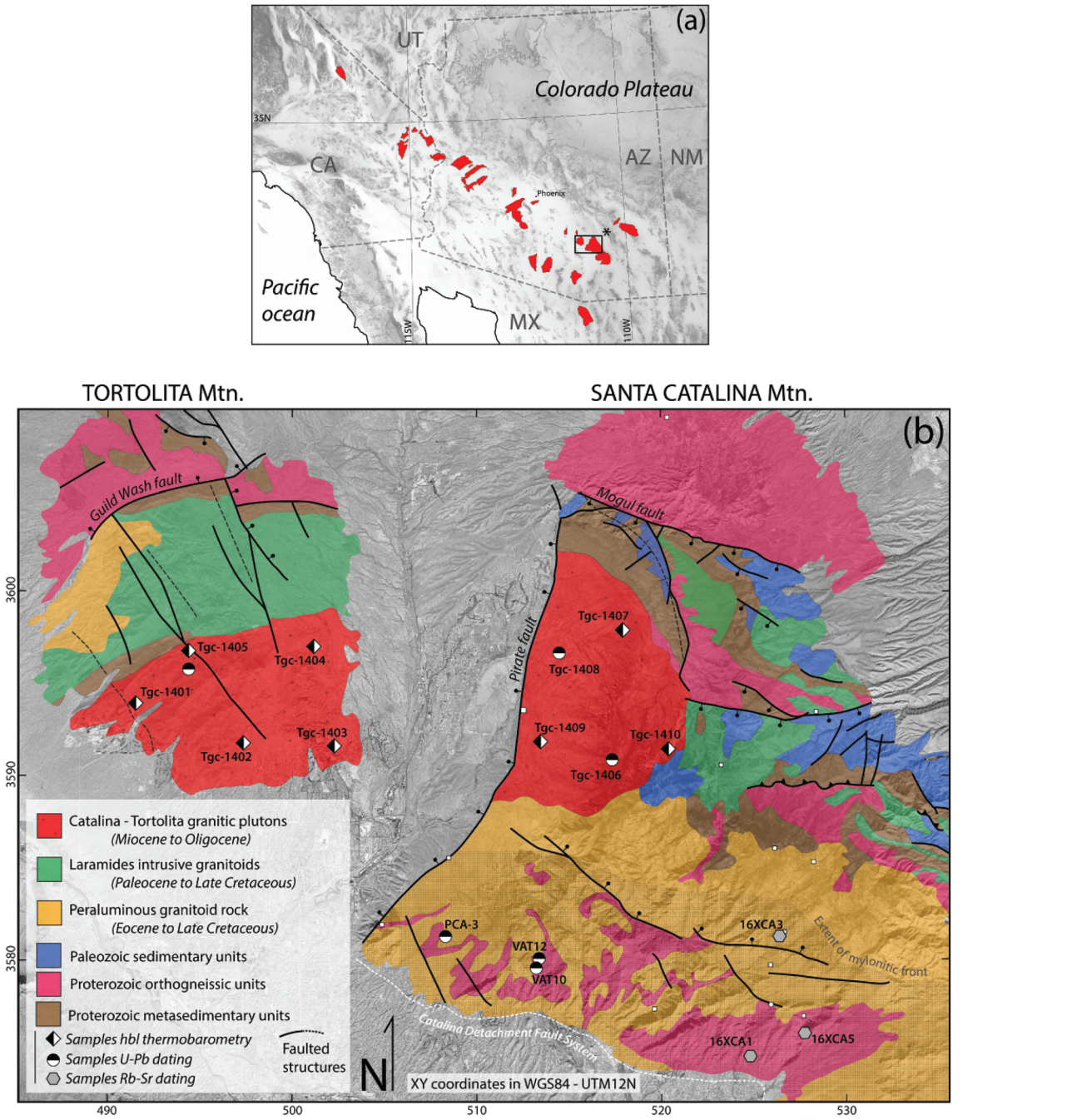

Figure 1. Location maps (a) geographic distribution of SW US metamorphic core complexes (MCC) (modified after Keith et al., 1980) and location of Figure 1b. (b) Simplified geologic map of the Catalina-Tortolita region and its MCC showing major geologic units and major faults (modified after Dickinson, 1991 and Fornash et al., 2013). Gray shading shows the extent of predominantly top to the SW augen gneisses and mylonites in the Catalina forerange. Locations of samples analyzed in this study are also shown.

of the term and development of concepts), MCCs have since been recognized worldwide in virtually all Phanerozoic orogens. However, MCCs can differ locally in terms of the geometry of the hanging wall, involvement of partially molten crust, magnitude of exhumation, and depth of extensive kinematics (Whitney et al., 2013). Thermal pulses resulting from magmatic intrusions synchronous with extension have been suggested as alternative modes of formation for these ductile detachment systems, at much shallower levels (Lister & Baldwin, 1993; Spencer et al., 1995). Moreover, older ductile fabrics are

demonstrably present in many MCCs, and this leaves one major question still unresolved: Are mylonitic fabrics coeval with large magnitude extension and MCC development, or do they reactivate pre-existing weaknesses in the crust?

We address some of these outstanding issues on the well-studied Catalina MCC. Here we present new zircon U-Pb and muscovite and biotite Rb-Sr isochron geochronology together with Al-in-hornblende igneous barometry on the Catalina MCC to get a better understanding of the temporal link between ductile deformation, depth of deformation, and magmatism. We show that the principal ductile fabric was formed during the Eocene in the presence of abundant magmatic syn-kinematic dikes as well as the presence of several large sills that add about 4 km to the thickness of the exposed section (Fornash et al., 2013). Overall, the Catalina Detachment Fault is a much shallower structure than most commonly accepted and significantly younger than the principal mylonitic fabric. These results are questioning the major connection between the ductile fabric and the low-angle detachment system and provide a first step toward a future in-depth petrochronological study of the evolution of the Catalina MCC.

1.1. Geologic Background and Samples

This study focuses on the Catalina and Tortolita Mountains of the Catalina-Rincon-Tortolita MCC (Figure 1a). Several samples for igneous thermobarometry and zircon U-Pb chronology were collected from the Catalina Intrusive Suite in the western Catalina Mountains and the Tortolita Mountains (see below), as well as from a vein located in the forerange of the Catalina Mountains from the mylonite zone. Rb-Sr chronology was performed on three samples from the forerange mylonites (Figure 1b). We briefly describe the regional geology, followed by a list of the relevant geologic units (Catalina Intrusive Suite and the forerange mylonite) that were sampled for this study. For more detailed descriptions of regional geology, we refer the reader to DuBois (1959), Keith et al. (1980), Spencer and Reynolds (1989), or Dickinson (1991), and Spencer et al. (2019).

1.1.1. Geologic Background

The Tortolita-Catalina-Rincon (or Catalina) MCC is one of the largest in an east-west oriented chain of MCCs from southern California through southern and central Arizona MCCs. Discovered in the 1970s, the Catalina MCC was among the first MCCs described in the world (Figure 1a; Crittenden et al., 1980; Davis & Coney, 1979). The Catalina MCC exposes a footwall in the Catalina Mountains consisting of pervasively mylonitized granitoids of various ages (Figure 1b). Above the mylonitic zone, a low-angle brittle fault, referred to as the Catalina Detachment Fault, separates the footwall rocks from the hanging wall comprising the Tucson basin and the Tucson Mountains to the southwest. Extension started at 26.4 Ma, as constrained by a high precision Ar-Ar tuff age in the Cienega Basin, at the base of the Rincon Mountains (Peters et al., 2003). If the Tucson Mountains restore to the top of the Catalina Mountains, as estimated by Dickinson (1991) among others, a ~40 km horizontal displacement exists along this low-angle detachment system, which is well within the range of such numbers estimated elsewhere in the Basin and Range (Wernicke, 1985). The rocks of the footwall are Precambrian Pinal Schist (1.65 Ga) and parts of a large anorogenic intrusion, the Oracle Granite (1.45 Ga), minor Paleozoic and Mesozoic rocks at least on the south side of the Catalina Mountains, and three distinctive plutonic products of the latest Mesozoic into the latest Oligocene: the Leatherwood Intrusive Suite, the Wilderness Sills Suite, and the Catalina Intrusive Suite (Keith et al., 1980). The Leatherwood Suite comprises small volume of Laramide plutons (65–72 Ma) (Fornash et al., 2013; Keith et al., 1980; Terrien, 2012), ranging from quartz-diorite to granodiorite in composition and distinctive in that, in addition to hornblende and biotite, they contain relatively abundant primary epidote. The "Wilderness Sills" Suite represents a series of at least eight major leucrogranitic two-mica and garnet-bearing sills (57–45 Ma) that add to more than 4 km crustal thickness (Fornash et al., 2013; Keith et al., 1980; Terrien, 2012), to which countless of minor sills and dikes found throughout the Catalina Mountains are also attributed. The Wilderness Sills Suite is two mica and garnet-bearing S-type leucocratic granitoids. The Wilderness Sills Suite units also contain metamorphic zircons and monazites dated between 45 and about 34 Ma (Terrien, 2012), suggesting that they underwent high-grade supra- to relatively hot subsolidus conditions for ~12 Myr after their magmatic emplacement. The Catalina Intrusive Suite (27–25 Ma, Shakel et al., 1977, Keith et al., 1980, and references therein, Fornash et al., 2013, and this study) comprises a distinctive group of quartz-diorite, quartz-monzonite to granodiorite intrusions found in the NW of the

Catalina Mountains as well as the Tortolita Mountains. The Catalina Intrusive Suite is largely undeformed in the Catalina Mountains exposures but partly mylonitized in the Tortolita Mountains.

While in the Catalina Mountains region, the Wilderness Sills Suite rocks are among the dominant intrusive rocks found in outcrop, regionally in SE Arizona, rocks of the Catalina Intrusive Suite age far exceed in volume the other latest Mesozoic and Cenozoic pulses of magmatism. More than 50% of the surface exposure of nonbasin fill rocks of SE Arizona are represented by volcanic rocks (and some, less abundant intrusive equivalents) of the so-called ignimbrite flare-up of the latest Oligocene. These late Oligocene ignimbrites represent a volume estimated to be over 1 million km^3. Regionally they range in age from 40–25 Ma (Best et al., 2016) and locally from 28–26 Ma in southern Arizona (Dickinson, 1991). While its origin is still debated, the ignimbrite flare-up was a magmatic event of extraordinary significance regionally across the American southwest and northern Mexico. Volcanic rocks of ages equivalent to the Catalina Intrusive Suite and belonging to the great ignimbrite flare-up are most closely found in the Tucson Mountains as relatively small volume units and the Galiuro Mountains to the north of the Catalina Mountains, where they are up to 2 km thickness in places.

The forerange of the Catalina Mountains consists of a 1- to 2-km thick tectonic complex and magmatic patchwork made of mylonitic gneisses, augen gneisses, and finer grained deformed metamorphic rocks located directly below the Catalina Detachment Fault (Figure 1b). Penetrative deformation of the paragneiss was associated with upper greenschist-grade to locally lower amphibolite-grade metamorphism, with metamorphic minerals including talc, tremolite, diopside, phlogopite, biotite, muscovite, cordierite, and K-feldspar (Lingrey, 1982). Keith et al. (1980) demonstrated that there were three distinct ductile deformation events (mylonite forming): one during the Latest Cretaceous, one Eocene, and one that is latest Oligocene. Which one is the dominant fabric, if any, is not specified in Keith et al. (1980) nor is it resolved by later contributions. Mylonite protoliths mainly consist of former intrusive granitic units. It is difficult to identify and distinguish among different possible "granitic" protoliths based on field evidence alone. The shallowly dipping mylonitic foliations strike predominantly WSW (Davis & Coney, 1979; Davis, 1980) and bolster the idea that the brittle detachment system and the mylonite were active geologically at the same time. The hanging wall is thought to be exposed in the Tucson Mountains to the SW of the detachment system, while in between, the Tucson Basin received early Miocene-modern fluvial sediments predominantly from the nearby Catalina Rincon Range. The mylonite zone is cut by small basaltic dikes of age 20 Ma or younger (Keith et al., 1980); thus the early Miocene must be the latest time of development of the ductile fabric. The mylonite is dominated in places by augen gneissic formations (former Oracle Granite), along with other felsic orthogneissic units, derived from the Wilderness Sills Suite materials, predominantly in this shear zone. Ductile deformation of quartz and the brittle truncation of feldspars are particularly well observable in Rapakivi texture of the Oracle augen orthogneiss. The combination of these deformation modes has made researchers postulate that the temperature range of deformation was around 350–450°C (Spencer et al., 1995) throughout this MCC. In detail, any of the of forerange canyons contain well exposed areas where it is difficult to explain every single lithologic variety—rocks resembling the 1.1 Ga dikes are found locally as well as rocks similar to the Pinal Schist. Given the degree of transformation of the fabric, a positive identification of some of these rocks is often difficult in the field. Leucocratic veins (of obvious magmatic origin) having thicknesses from cm to tens of meters, crosscut and in places run concordant with the main foliation of the mylonite. They represent as much as 40–60% of the local outcrop making the identification of protoliths even more complicated. Their grain sizes can strongly vary locally, from medium grain to coarse pegmatitic texture. Some of these dikes are deformed; others show very little to no internal deformation. Overall, most researchers agree that these leucocratic rocks are late kinematic with respect to the development of the main mylonitic foliation, and their age has to constrain the end of mylonitic fabric development (Anderson et al., 1988; Keith et al., 1980). Despite these complexities at outcrop scale, it is clear that there are two rock types that dominate the mylonite zone: The Oracle Granite deformed into a distinctive augen gneiss and finer mylonitic varieties and the Wilderness Sills Suite, both displaying the dominant top to the SW sense of shear. The principal ductile deformation is thus Eocene or younger. No zircon U-Pb age data exist on any of the dikes that could constrain the age of deformation.

The Catalina Intrusive Suite is locally mylonitized forming what is volumetrically a small subset of the exposed mylonite volume in the Tortolita Mountains. This clearly demonstrates that some of the ductile

deformation must be latest Oligocene or Miocene (Keith et al., 1980, for a summary). The Catalina Intrusive Suite may be locally deformed by ductile shear zones in its *locus typicus* in the Catalina Mountains; however, for the most part it sits below the mylonite front of the forerange of the Catalina Mountains (Dickinson, 1991).

The main part of the Catalina Intrusive Suite is exposed as a semicircular pluton in map view in the northwestern Catalina Mountains and is located about 1 km structurally beneath the Catalina Detachment Fault (Dickinson, 1991). The geometric relationship between the main mylonite and the Catalina Intrusive Suite is affected by subsequent normal faults that break down the otherwise relatively simple anticlinorium shape of the Catalina range. The Catalina Intrusive Suite is also found in the hanging wall of a later Basin and Range fault called the Pirate Fault, in the Tortolita Mountains to the west of the Catalina Mountains (Figure 1b). Colloquially referred to as the "Catalina Granite," these plutonic rocks are compositionally diverse, most commonly quartz monzonites, tonalites, and granodiorites with only minor granite *sensu stricto* (Keith et al., 1980, our field observations) with initial $^{87}Sr/^{86}Sr$ ratios of 0.708–0.709. They are I-type granitoids, in sharp contrast to the earlier Wilderness Sills Suite, which are S-type granites. There are clearly several distinctive intrusive events that were identified in the earlier field-based petrographic studies of the area (summary in Keith et al., 1980) which makes the Catalina Intrusive Suite an assemblage of successive pluton emplacement of close but not identical ages. As deduced from exposures, the Catalina Intrusive Suite is at least 12 km in diameter horizontally and at least 1.2 km thick based on its exposures, probably much more, given that another circular body of the same intrusive suite about 3 km in radius crops out in the Tortolita Mountains. It is likely that larger equivalents exist at depth throughout much of the Catalina forerange, not much below the present surface (Terrien, 2012).

1.1.2. Sample Descriptions

Ten samples were collected for igneous thermobarometry from the Catalina Intrusive Suite, five from the northwest Santa Catalina Mountains, and five from the Tortolita Mountains. Sample locations are given in supporting information Data S1 and displayed in Figure 1b. Thin sections of each sample were made, and petrographic analysis determined that five of the samples had the quartz + alkali feldspar + plagioclase + hornblende + biotite + iron titanium oxide + titanite mineral assemblage required for the use of the aluminum-in-hornblende thermobarometer.

Three of the samples used for thermobarometry, one from the Tortolita Mountains and two from the Catalina Mountains, were used for U-Pb zircon geochronology (Tgc-1405, Tgc-1406, and Tgc-1408). They all consist of coarse undeformed granodiorites with biotite and hornblende and also contain accessory zircon, magnetite/hematite, apatite, and titanite.

Three additional samples were collected in the forerange mylonitic zone. They represent two dikes that are syn- to late kinematic, only slightly deformed and include boudinaged granitoids from Ventana Canyon (VAT10 and VAT12, Figure 2) and one undeformed biotite-leucogranitic dike from Pima Canyon (PCA3). Their location is given in Data S2 and Figure 1b. At the thin section scale, there is no deformation in any of the analyzed samples (Figure 3). Planar fabrics of the Ventana Canyon are only vaguely distinctive in outcrop. These dikes intrude the Oracle granitoid suite deformed and metamorphosed into a mylonitic augen gneiss with top to the SW shear sense indicators. Sample VAT10 consists of a medium to coarse grained leucogranite (quartz + plagioclase + K-feldspar + biotite ± muscovite ± garnet) with a diffuse planar fabric due to ductile deformation. It occurs as pluri-centimetric to metric dike network crosscutting the host gneiss foliation (see Figure 2). Contacts between the dikes and the host highly foliated gneiss are marked by irregular cauliflower structures. Sample VAT12 is petrographically similar to VAT10. It is a two-mica leucogranitic dike, showing slightly oriented coarse to pegmatitic texture and appears to have intruded later than VAT10 in a relative sense, since it is more obliquely crosscutting the Oracle gneissic foliation. These dikes are pseudo-boudinaged, marked by pluri-millimetric biotite-rich selvedges and cauliflower contacts with the host augen gneiss which suggest syn- to late tectonic emplacement. Sample PCA3 consists of an undeformed medium-grained (and locally pegmatitic) leucogranite made of quartz + plagioclase + K-feldspar + titanite ± biotite. It crops out as an anastomosed network of centimetric to metric dikes crosscutting with sharp contacts the Oracle meta-diorite gneissic foliation, which at this location displays a top to the SW sense of shear.

Three additional samples were collected for Rb-Sr geochronology. Their location is given in Data S3 and Figure 1b. Sample 16XCA1 is a mylonitic Oracle Granite from Pima Canyon, which contains both biotite

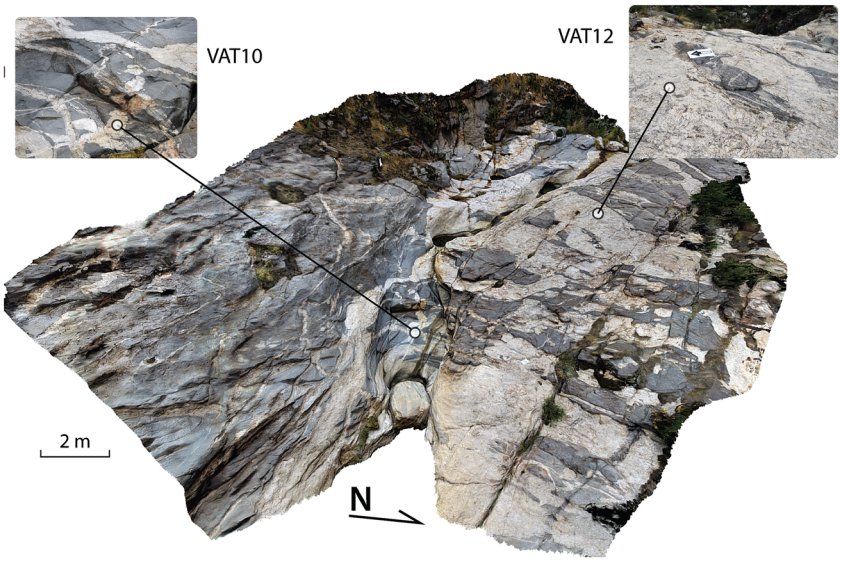

Figure 2. Field view of Eocene two-mica leucogranites (light colors) VAT10 and VAT12 (Ventana canyon) intruded into Oracle augen gneiss (darker color). Host gneisses (mylonitic) are crosscut by medium-grained leucrogranitic dikes (VAT12), then, crosscut by "granitic" dikes (VAT10) that are undeformed. A third generation of undated (also two mica-bearing) dikes further crosscuts the mylonitic fabric.

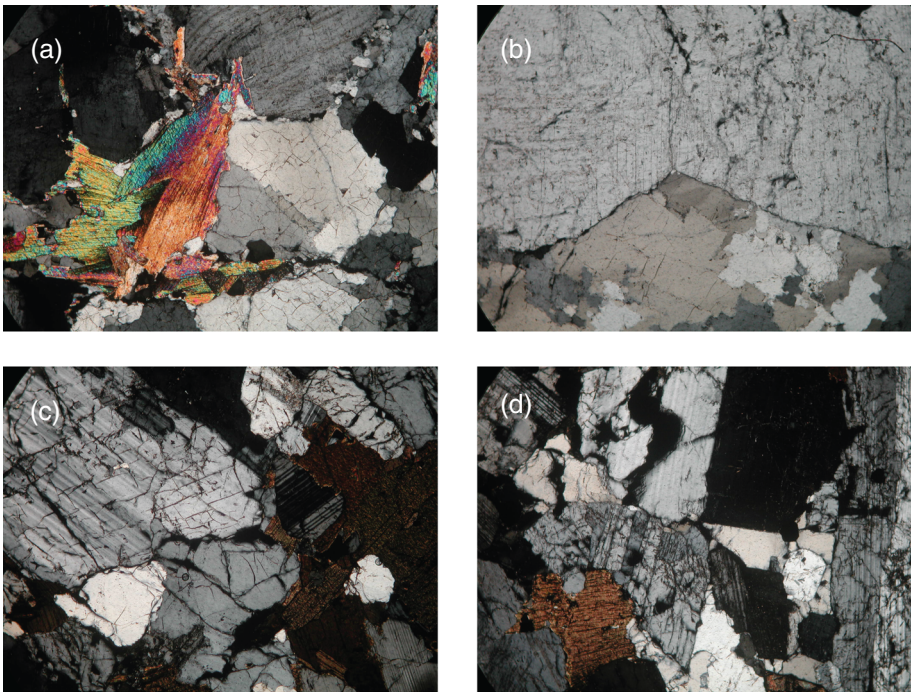

Figure 3. Cross-polar microphotographs of leucogranitic dikes; long dimension (horizontal) field of view is 1 cm in each photo. Note the lack of internal deformation in any of the images. (a) Two mica leucogranite VAT10; (b) large K-feldspar and quartz with 120^0 grain boundaries in VAT12, (c) and (d) plagioclase, quartz, biotite, and lesser amounts of K-feldspar in granitoid PCA3.

and muscovite, perhaps due to small scale solid mixing with a younger leucocratic vein, whereas the other two samples (16XCA3 and 16XCA5) are mylonitic Wilderness Sills Suite two-mica granites from the forerange of the Catalina MCC along the Catalina Highway (Figure 1b).

2. Methods

2.1. Aluminum-in-Hornblende

We use the aluminum-in-hornblende thermo-barometer (calibration of Anderson & Smith, 1995) coupled with the hornblende-plagioclase thermometer (Blundy & Holland, 1990) to estimate the depth and temperature of the emplacement of the Catalina intrusive suite (using the updated algebra from Anderson et al., 2008). Chemical analysis of plagioclase-hornblende pairs was performed using a CAMECA SX100 electron microprobe at the University of Arizona, and the total aluminum content of the hornblende grains was determined through formula recalculation of the microprobe data as outlined in Leake et al. (2004). Representative compositions are given in Data S1.

2.2. Zircon U-Pb

The zircons from each sample were extracted using the traditional method of crushing, sieving, heavy liquid separation, magnetic separation, and hand-picking. The ~40 zircon grains from each sample were then mounted on epoxy with SL, R33, and FC zircon grains used as primary and secondary standards (see detailed method and analytical procedure in Pullen et al., 2018). Growth features and morphology of each zircon grains were identified using cathodoluminescence (CL) images using the Gatan ChromaCL2 scanning electron microscope in the Arizona LaserChron SEM Lab. Spots for analysis were then picked using the CL images to locate core and rim boundaries in complex zircons. In situ isotopic analysis of the zircons was conducted using the Thermo Element2 single-collector inductively coupled plasma mass spectrometry (ICPMS) coupled to a Photon Machines Analyte G2 excimer lasers at the Arizona LaserChron Center (ALC) (Gehrels et al., 2006, 2008; Gehrels & Pecha, 2014). The U-Pb age for each analysis was then calculated using the ALC in-house software *E2agecalc*, and for concordant subsets, a weighted average age was calculated using *Isoplot 4.15* (Ludwig, 2008).

2.3. Muscovite and Biotite Rb-Sr Chronology

Plagioclase, biotite, and muscovite were measured for mineral Rb-Sr thermochronology on three samples at the Arizona TIMS laboratory. The analytical procedures followed Otamendi et al. (2009), Drew et al. (2009), and Toljić et al. (2013). Minerals that were believed to yield a good spread on two-point Rb-Sr isochrons with the whole rocks were separated using a Dremel milling tool and using a Micromill instrument (see Ducea et al., 2003; Erak et al., 2017); both of these were equipped with Brassler burrs. The isotopic ratios of $^{87}Sr/^{86}Sr$ and the trace element concentrations of Rb and Sr for the mineral separates were measured by thermal ionization mass spectrometry. Powders were put in large Savillex vials and dissolved in mixtures of hot concentrated HF-HNO_3. The dissolved samples were then spiked with the Caltech (unmixed) Rb and Sr spikes (Ducea & Saleeby, 1998) after dissolution. Rb and Sr were separated in cation columns containing AG50W-X4 resin, using 1N to 4N HCl. Rb was loaded onto single Re filaments using silica gel and H_3PO_4. Sr was loaded onto single Ta filaments with Ta_2O_5 powder. Mass spectrometric analyses were carried out at the University of Arizona on an automated VG Sector multicollector instrument fitted with adjustable 10^{11} Faraday collectors and a Daly photomultiplier (Otamendi et al., 2009). Concentrations of Rb and Sr were determined by isotope dilution with isotopic compositions determined on the same spiked runs. An off-line manipulation program was used for isotope dilution calculations. Typical runs consisted of acquisition of 100 isotopic ratios. The mean result of five analyses of the standard NRbAAA performed during the course of this study is $^{85}Rb/^{87}Rb = 2.61312 \pm 17$. Five analyses of NIST standard NBS987 yielded mean ratios of $^{87}Sr/^{86}Sr = 0.710254 \pm 4$ and $^{84}Sr/^{86}Sr = 0.056436 \pm 12$. The Sr isotopic ratios of standards and samples were normalized to $^{86}Sr/^{88}Sr = 0.1194$. The estimated analytical $\pm 2\sigma$ uncertainties for samples analyzed in this study are $^{87}Rb/^{86}Sr = 0.15\%$ and $^{87}Sr/^{86}Sr = 0.0010\%$. Procedural blanks averaged from five determinations were Rb-5 pg and Sr-110 pg.

Table 1
Summary of Thermobarometry Results on Catalina Intrusive Suite

Sample	Pressure (GPa)	Error ±	Depth (km)	Temperature (°C)	Error ±
Tgc-1405	0.22	0.06	8.0	672	22
Tgc-1406	0.20	0.06	7.3	682	26
Tgc-1407	0.17	0.07	6.3	661	29
Tgc-1408	0.13	0.07	4.7	638	36
Tgc-1409	0.14	0.08	5.2	670	40

3. Results

3.1. Thermobarometry

All amphibole grains consist of calcic amphibole with magnesiohornblende/edenite composition (0.14 to 0.51 $[Na + K]^{[A]}$ apfu for 6.5 < $Si^{[iv]}$ apfu < 7.4 and 57 < Mg# < 87 mol.%) (Leake et al., 2004). Total aluminum content in the hornblende grains range between 0.65 to 1.80 apfu (atom per formula unit). Plagioclases are unaltered and show oligoclase to albitic primary compositions, with xAb (=Na/[Na + Ca + K] apfu) ranging from 0.70 to 0.88. In-contact amphibole-plagioclase pairs were used for temperature equilibrium estimates (see Data S1).

Results from the aluminum-in-hornblende barometer indicate average pressures to be 2.2 ± 0.6 kbar, 2.0 ± 0.6 kbar, 1.7 ± 0.7 kbar, 1.3 ± 0.7 kbar, and 1.4 ± 0.8 kbar for samples Tgc-1405, Tgc-1406, Tgc-1407, Tgc-1408, and Tgc-1409, respectively. Corresponding depths of emplacement are calculated to be 8.2, 7.5, 6.5, 4.8, and 5.4 km, using an average density of 2,690 kg/m^3. These results are similar to those reported by Anderson et al. (1988). There is no obvious spatial pattern for these paleodepths; there is only some consistency in that they are low numbers: The combined average depth is 6.45 km. All samples were collected from more or less the same depth within the intrusive suite—covering about 500 m of the total range of 1.2 km thickness. Al-in-hornblende barometry is a moving target, since amphibole locks in its composition and pressure at various depths as the plutonic mass is moving upward; in that light, the most likely resting depth of the Catalina Intrusive Suite is the lowest value measured, around 5 km beneath the surface. Average hornblende-plagioclase temperature of emplacement is calculated to be 672 ± 22°C, 682 ± 26°C, 661 ± 29°C, 638 ± 36°C, and 670 ± 40°C for samples Tgc-1405, Tgc-1406, Tgc-1407, Tgc-1408, and Tgc-1409, respectively (Table 1).

3.2. Zircon U-Pb Chronology of the Catalina Intrusive Suite

Weighted ^{238}U-^{206}Pb ages for the Catalina Intrusive Suite, with uncertainty reported at 2σ, are 24.85 ± 0.14 Ma, 24.79 ± 0.16 Ma, and 25.04 ± 0.15 Ma for samples Tgc-1405, Tgc-1406, and Tgc-1408, respectively (Figure 4). Corresponding MSWD's (mean square weighted distribution) are 1.7, 3.9, and 2.7. There is no significant difference in age between rims and cores of complex zircon grains. At least 25 grains were measured for each sample for the reported age. A combined weighted U-Pb age including all samples was calculated to be 24.91 ± 0.12 Ma, with a corresponding MSWD of 2.6. This age is consistent with the previously reported age range of 23–27 Ma (summarized in Dickinson, 1991) and slightly younger than a previous zircon U-Pb age of 25.8 + 0.4/−0.5 Ma (Fornash et al., 2013). Our individual grains pooled for an average age do span an age range from 27 to 24 Ma, and we cannot assess concordance on ages that are young enough such that only $^{206}Pb/^{238}U$ ages are reliable. It is very likely that the Catalina Intrusive Suite (which was never mapped in great detail to identify plausible multiple batches of magma) was built in small increments over more than 1 or close to 2 Myr. This is unlike the earlier local episode of magmatism represented by the long-term emplacement of the Wilderness Sills Suite (57–45 Ma, with continued monazite and metamorphic zircon growth until 34 Ma, Terrien, 2012), for which there is evidence that individual sills were above or close to the solidus for several million years.

3.3. Zircon U-Pb Chronology of Intrusive Dikes in the Southern Mylonitic Zone

Sample VAT10. Zircons are 200 to 500 μm long, prismatic, colorless showing euhedral shape with sharp edges. Based on CL images, they show regular oscillatory zoning, suggesting magmatic crystallization

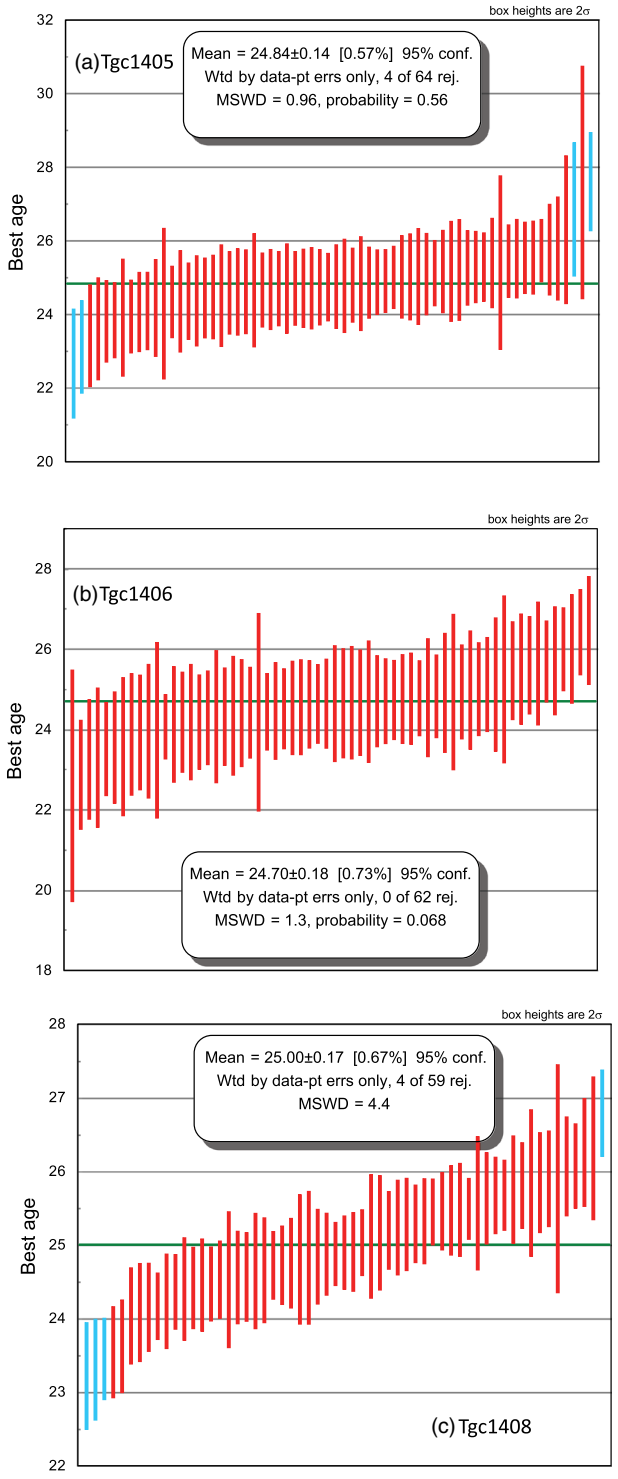

Figure 4. Zircon ^{238}U-^{106}Pb ages Catalina intrusive suite rocks with MSWD and errors. Red lines (individual ages and their errors) are used in the average calculated age, whereas the blue outliers are not.

(Figure 4). U-Pb isotopic data ($n = 20$) point to an Eocene age, with weighted mean of best ages at 46.6 ± 0.8 Ma, with an MSWD of 2.3 (Figure 5).

Sample VAT12. Extracted zircons are >150 μm long, colorless, and euhedral. In situ isotopic data ($n = 20$) also point to an Eocene age. Weighted mean of U-Pb concordant ages spotted an age of 46.9 ± 1.0 Ma, with an MSWD of 2.8 (Figure 5).

Sample PCA3. Zircons are 50 to 200 μm long and show CL highly luminescent xenocrystic cores surrounded by poorly luminescent overgrowths (Figure 6) marked by regular oscillatory zoning. U-Pb isotopic results of zircons' cores are strongly spread (MSWD = 255, $n = 18$) due to a lead loss episode. The isotopic data show a discordant alignment yielding an upper intercept age pointing to a poorly constrained Late Paleoproterozoic age (1659± 52 Ma; Figure 6). U-Pb data from zircons' rims point to an Oligocene age. Most analyses are concordant, and weighted means of $^{235}U/^{207}Pb$ ages spotted an age of 25.5 ± 0.4 Ma (Figure 6). Zircons are magmatic, as evidenced by their U/Th ratios of less than 5 (Table 2).

3.4. Rb-Sr Chronology

All three samples have almost identical ages within error. Muscovite-plagioclase pairs yield ages of 33.9 ± 0.1 Ma (16XCA1), 33.5 ± 0.07 Ma (16XCA3), and 34.2 ± 0.08 Ma (16XCA5). Sample 16XCA1 has an age-corrected $^{87}Sr/^{86}Sr$ of 0.74505 (at 34 Ma) which is typical of the 1.455 Ga Oracle Granite at the 34 Ma time mark. The other two samples have age corrected of 0.71122 (16XCA3) and 0.71259 (16XCA), which are typical of the much younger (57–45 Ma) Wilderness Sills Suite rocks. Biotite-plagioclase pairs yield ages of 24.7 ± 0.2 Ma (16XCA1), 24.8 ± 0.07 Ma (16XCA3), and 26.0 ± 0.1 Ma (16XCA5) (Table 3).

Closure temperature is difficult to assess in the case of Rb-Sr system (see Muller, 2003, for discussion) for many minerals and especially micas, with few reliable diffusion data available. In general, amphibole, feldspars, epidote, and white micas close around 500–600°C (Freeman et al., 1997), whereas biotite has a much lower closure temperature, 250–350°C (Dodson, 1973), although closure depends significantly on grain size and cooling rate. More importantly, the degree of recrystallization during ductile deformation may reset the white micas system more than closure temperatures in highly deformed rocks that experienced ductile shear in the midtemperature range (300–500°C) (Eberlei et al., 2015; Villa, 2016). Based on the large crystal size (0.5–1 cm), and the above-mentioned diffusion data, we estimate that the closure temperature was around 400–450°C for muscovite and around 280–320°C for biotite analyzed in this study. For muscovite, the temperature range broadly coincides with the range of ductile deformation temperatures based on mineral assemblages in the mylonite (Lingrey, 1982); consequently, we interpret that the muscovite-plagioclase white mica Rb-Sr ages may date the termination of ductile deformation and metamorphism. Biotite, on the other hand, given its lower closure temperatures, is more likely to have closed to the Rb-Sr system in a fashion suggested by the classic closure temperature concept, at around 300°C in this case.

4. Discussion

4.1. Relationship Between the Main Ductile Fabric and Dikes

The principal mylonitic fabric comprises the augen gneissic and mylonitic textures on the Oracle granitoids and the Wilderness Sills Suite in the forerange of the Catalina and Rincon Mountains. The fabric is

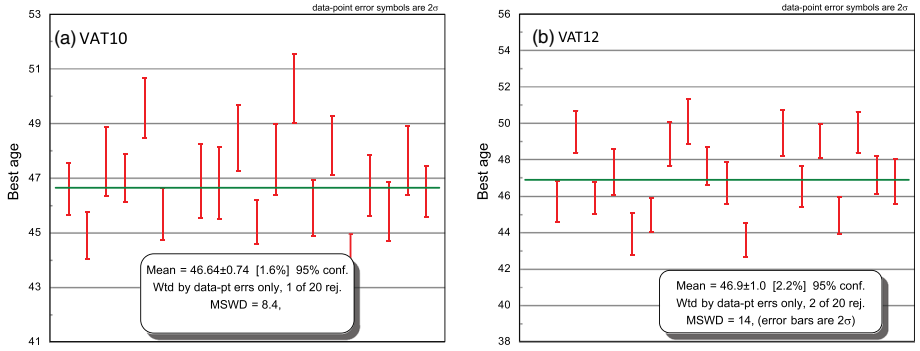

Figure 5. Zircon ^{238}U-^{106}Pb ages of dikes VAT10 and VAT12 with MSWD and errors. Analyzed spots represent cores and rims of zircon grains. All values were used in pooling the average age.

pervasive, is oriented top to the WSW in most places, and is particularly easy to follow in the gray colored biotite-bearing Oracle Granite rocks, whose undeformed equivalents are well described outside of the mylonite zone. These deformed Oracle Granite rocks are pervasively invaded by veins of magmatic origin, ranging in thickness from centimeter to several meters. The anastomosing felsic veins make up as much as 40–60% of outcrops in some of the canyons of the forerange of the Catalina Mountains. Yet they are not migmatites; there is no evidence that the metamorphosed package of the forerange has been subjected to more than upper greenschist or maybe the lower most amphibolite grade (Lingrey, 1982).

There are two types of leucocratic veins and dikes (all referred to as dikes for simplicity): (1) 46–48 Ma, S-type two mica and garnet-bearing leucocratic granites most commonly pegmatitic in texture and (2) 25–26 Ma, I-type biotite granodiorites. We studied two samples of the first group (VAT10 and VAT12) and one of the second group (PCA3). Both crosscut the foliation, but the second type is clearly post kinematic at outcrop scale (Figure 2) and shows no internal deformation in thin section (Figure 3). The first type shows complex patterns (Figure 2) including alternating concordant areas with domains that are clearly crosscutting the main Oracle Granite mylonitic foliation. This earlier type of leucogranite also has very little to no internal deformation at the thin section or hand specimen scale (Figure 3) but display in places, some weak banding at the 10 cm scale. We interpret these as being late kinematic. An additional view of the outcrop-scale geometry and the relationship between dikes and the mylonitic foliation is provided in two photographs from the sampling area for U-Pb geochronology (Figure S1) where the mylonitic foliation was traced on the images. The complex but clearly crosscutting S-type granitoids can only be either syn-kinematic or late

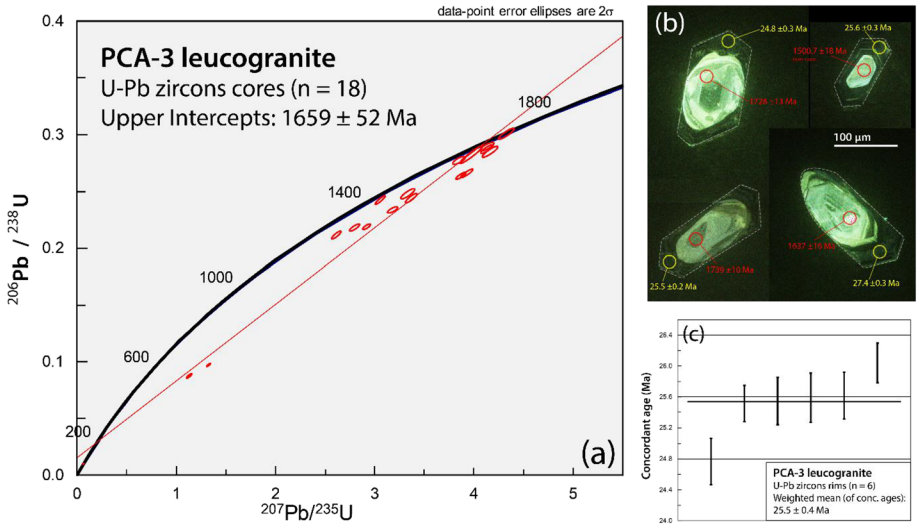

Figure 6. (a) Zircon U-Pb Concordia diagram for the PCA-3 sample. (b, c) Cores have inherited Proterozoic ages, whereas rims have a latest Oligocene age (25.5 ma) interpreted to represent crystallization age.

Table 2
Summary of Zircon U-Pb Ages

Sample	Crystallization age	Error	MSWD	Inherited ages
Tgc-1405	24.84	0.14	0.96	
Tgc-1406	24.70	0.16	1.3	
Tgc-1408	25.00	0.17	4.4	
VAT10	46.6	0.7	8.4	
VAT12	46.9	1.0	14	
PCA3	25.5	0.4	9.7	1,659 ± 52

kinematic with respect to the foliation. Given the abundance of quartz in both of these types of rocks (which are granites), one would expect that the ductile deformation in quartz should be as intense if not more in these rocks if they were prekinematic with respect to the principal mylonite fabric which they crosscut, a hypothesis that is ruled out here.

4.2. Oligocene Cooling

The Eocene age of late to syn-kinematic felsic dikes in the forerange mylonitic zone establishes clearly that the main ductile fabric was acquired during the Eocene and not late Oligocene. This has been speculated in various forms in the past, mostly by some who suggested that the fabric progressively developed over a long term including the early to mid-Cenozoic but also the latest Oligocene (Crittenden et al., 1980; Keith et al., 1980). Our new data put some important constraints toward firmly establishing an early Eocene age for the mylonitization deformation event, synchronous with the emplacement of the Wilderness Sills Suite. Does that mean that extensional fabrics and extension started earlier in the region? The dominant top to the south and west-striking fabrics as evidenced by shear sense indicators in present coordinates may simply reflect a subhorizontal ductile flow at the time of fabric development since it is parallel to the orientation of the larger Wilderness Sills. These were rotated during the latest Oligocene low-angle extension and to some extent also in response to emplacement of the Catalina Intrusive Suite to take the overall domal shape of the Catalina Mountains structure. It is plausible that the brittle fabric and development of the Catalina detachment system exploited the earlier fabric hence their common orientations. It has already been demonstrated in the Rincon part of the system that the Oligocene-Miocene detachment system exploited the rheological weaknesses of a former Laramide thrust system (Spencer et al., 2019).

White mica Rb-Sr ages imply that temperatures remained hot (400–450°C) in the studied section until 34 Ma. We interpret this age to be the result of cooling of the section following the end of protracted magmatism and metamorphism that lasted into that age range. While the Wilderness Sills Suite rocks are believed to be no younger than about 40 Ma, and mostly in the 57–45 Ma, (Fornash et al., 2013; Terrien, 2012), numerous zircons and monazites with questionable metamorphic signatures have grown in these rocks in the 35–40 Ma age range (Terrien, 2012; Gehrels, oral communication, 2019). Plutons of that age (34 Ma) do exist in the Rincon Mountains, and it is very likely that the Catalina section remained in a hot thermal regime with the sills possibly being close to the solidus until the Eocene-Oligocene boundary. Our muscovite Rb-Sr data provide thermochronological arguments that the section started to cool below ductile deformation temperatures at the Eocene-Oligocene boundary. Anderson et al. (1988) calculated about 2–9 km of crustal exhumation between the emplacement of the Wilderness Sills Suite and the time of emplacement of the Catalina Intrusive Suite (either from 15 or 8 km to 6 km paleodepths, depending on which barometer is used). These numbers rest on the barometric estimates on the Wilderness Sills Suite which have large uncertainties. Most basin fill in the region is represented by latest Oligocene and Miocene rocks resting on various basement, and there are no more than 1–2 km thick sedimentary sections of Oligocene (Dickinson, 1991, and references therein); the lower end-member for the amount Eocene to Oligocene unroofing (2 km, Anderson et al., 1988) are consistent with independent observations from local geology. Therefore, the paleo-depth of the Wilderness Sills Suite exposed today needs to be re-examined for a definitive assessment of how much exhumation accompanied the cooling path between 34 and 25 Ma. In the meantime, while cooling through midtemperature thermochronometers is demonstrated for the 34–25 Ma interval with our Rb-Sr data and exhaustive Ar-Ar multidomain diffusion work (Terrien, 2012), the amount of exhumation associated with this cooling is yet to be quantified.

Table 3
Summary of Mineral Rb-Sr Ages

Sample	Muscovite-plagioclase age	Biotite-plagioclase age
16XCA1	33.9 Ma	24.7 Ma
16XCA3	33.5 Ma	24.8 Ma
16XCA5	34.2 Ma	25.9 Ma

Note. Errors on Rb-Sr two-point isochrons are analytical and decay constant uncertainties only and are about 0.1 Ma or less for the reported ages.

4.3. Catalina Intrusive Suite

Our Catalina Intrusive Suite zircon ages average a relatively short interval at 24.9 ± 0.2 Ma, which is slightly younger than a previous estimate from the same laboratory (Fornash et al., 25.8 ± 0.5 Ma) but using a different instrument. Earlier conventional TIMS U-Pb zircon dating of the same pluton yielded a 27 Ma age (Shakel et al., 1977), whereas a host of

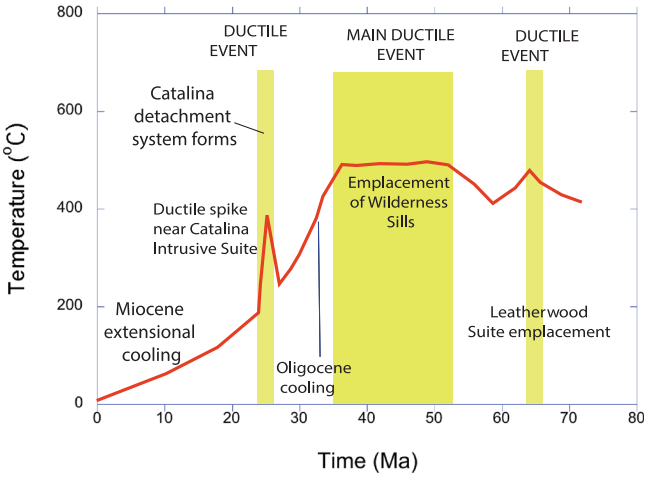

Figure 7. Proposed age temperature path for the Catalina region in the latest cretaceous and Cenozoic. Blue line represents the main path, whereas some areas may have undergone additional transient heating due to the emplacement of the Catalina intrusive suite.

radiometric age determinations in the 1980s yielded a range of 23.5 to 28 Ma (Keith et al., 1980; Reynolds et al., 1986). Our new data and Fornash et al. (2013) strongly suggest that the Catalina Intrusive Suite was emplaced at 25–26 Ma, synchronous with the Rb-Sr data marking beginning of their exhumation. A plethora of lower temperature chronometers (Fayon et al., 2000; Terrien, 2012) as well as the timing of accumulation of sediment in the Tucson basin document cooling and exhumation immediately after 25–20 Ma. The Catalina Intrusive Suite emplacement was thus contemporaneous with the development of the brittle normal fault system; its emplacement likely had an important role in doming the structure and shaping the orientation of the Catalina Detachment Fault. The 25 Ma dike in Pima Canyon establishes that magmatic input into the forerange mylonitic zone took place during the late Oligocene, synchronous and cogenetic with the Catalina Intrusive Suite, but it did so sharply crosscutting prior ductile mylonitic fabrics of the host. Nevertheless, a small fraction of the Catalina Intrusive Suite in the Tortolita and Catalina Mountains is described as plastically deformed, suggesting that relatively hot ductile (or transient ductile-brittle) deformation event did take place in the latest Oligocene along the margins of the plutonic suite (Keith et al., 1980).

4.4. Tectonic Implications

None of these data put a satisfactory constraint on tectonic and petrogenetic processes that took place between the timing of ductile fabric development and sills emplacement in the early Eocene and especially since the beginning of cooling in the latest Eocene and the late Oligocene. There is little extension and sedimentation documented prior to the latest Oligocene (Dickinson, 1991) and the amount of unroofing between 45 and 25 Ma is unresolved, largely due to lack of viable/reliable barometric assemblages for that purpose. We do know from this study that the crustal section currently exposed in the Catalina Mountains was relatively close to the surface at 25 Ma and that there is no unique solution to cooling or exhumation paths between 35 and 25 Ma, from Ar-Ar work (Terrien, 2012), or our Rb-Sr data (Figure 7).

At a larger scale, the most likely tectonic scenario for the area prior to extension-related cooling and exhumation is that the section currently exposed in the Catalina-Rincon mountains was an upper crustal part of the *Arizonaplano* plateau in the SW US (Chapman et al., 2020), similar to the modern Altiplano-Puna in South America (Garzione et al., 2017). As a high standing plateau, the area did not experience much erosion if at all, leading geothermal gradients in the crust to only increase over time. A consequence of that is the presence of long-lived intracrustal magmatism, some of which corresponds to partial melting of deeper metasedimentary assemblages. A subplateau environment is the most likely to preserve high temperatures of sills such as those making up the Wilderness Sills Suite for long periods of time, even if they were emplaced at relatively shallow levels in the crust. A good modern analog is the central Andean Plateau, where large magma bodies are known to exist under the modern Altiplano-Puna (Delph et al., 2017; Ward et al., 2017).

4.5. Regional Core Complexes and Eocene Magmatism

Our interpretations do not bear any information on other regional MCCs in which latest Oligocene or Miocene ductile deformation was firmly established, for example, the South Mountains MCC (Reynolds, 1985) or the Bucksin-Rawhide MCC (Singleton et al., 2014). Those do not contain the abundant Eocene plutonism of the Catalina MCC. We also do not question the high magnitude extension that took place at about 26 Ma and onward in the Tucson area and elsewhere in the Basin and Range province. The mechanism of unroofing along a low-angle detachment fault system is also not in question, and this high magnitude normal fault system led to the exposure of these MCCs. Prior to that, however, the American Southwest had a thick crust (Coney & Harms, 1984) and a long history of magmatism and relatively little compressional deformation or erosion documented at the latitude of the MCCs (Chapman et al., 2020). The geologic history from the latest Cretaceous and up to the extensional collapse of the latest Oligocene-Miocene is best documented where earlier Late Cretaceous or Cenozoic magmatism/

metamorphism is present (similar to how the Angel Lake area, East Humboldt Range, presents invaluable information with regard to Late Cretaceous crustal melting further north, McGrew et al., 2000). The Catalina MCC is one of the few MCCs of southern Arizona and eastern California that captures protracted early Cenozoic magmatism in the footwall of the MCC. Paleocene-Eocene magmatism in the 55–35 Ma age range is more common east of the Catalina MCC in easternmost Arizona and west New Mexico (NAVDAT.org). Sorting out earlier Cenozoic episodes of ductile deformation is critical in unraveling regional geology. We show here that the Catalina footwall developed its spatially most widespread penetrative ductile fabric prior to the latest Oligocene to Miocene extension.

5. Conclusions

Late kinematic quartzo-feldspathic dikes in the mylonite zone of the Catalina MCC are 46–48 Ma in age, synchronous with the emplacement of the Wilderness Sills Suite, a series of leucogranite sills (57–45 Ma and possibly later, metamorphosed into the latest Eocene, 34 Ma) (Fornash et al., 2013; Terrien, 2012) abundant in the Catalina Mountains. Much like the larger sills, these dikes are S-type granites with two micas commonly found in their mineral assemblage. The Eocene age is much older than the well-established (latest Oligocene) time of regional extension (Dickinson, 1991). Muscovite-plagioclase Rb-Sr ages are 34 Ma, probably marking the end of magmatism/high temperature deformation in the crust (Figure 7). These rocks were cooled below the 300–350°C isotherm at the time of emplacement of the Catalina Intrusive Suite (25 Ma), as evidenced by biotite-plagioclase Rb-Sr ages. Some post kinematic dikes of the Catalina Intrusive Suite age exist in the forerange mylonite as well. They are biotite granodiorites, are characterized by significant zircon inheritance of 1.6 Ga grains and have rims of late Oligocene age. Unlike the earlier, Eocene dikes in the fabric of the mylonite, they clearly crosscut the ductile fabric (are postkinematic) and are not S-type. To summarize, we interpret that all the abundant syn-kinematic and late kinematic leucrocratic material in the mylonite zone as S-type and synchronous with the Wilderness Sills Suite. All postkinematic crosscutting dikes are much less common that the previous types but are syn-Catalina Intrusive Suite (25–26 Ma) and are petrographically distinct from the earlier dikes.

The Catalina Intrusive Suite, located 1–2 km below the mylonite zone, formed at a depth of 6 ± 2 km beneath the surface based on Al-in-hornblende barometry. This estimate is in better agreement with the amount of material present in the nearby Tucson basin, suggesting that some 4 km of rock above the detachment rests today in the basin as latest Oligocene and Miocene and younger sedimentary rocks (Dickinson, 1991).

An attractive hypothesis reconciling shallow depth and ductile deformation was the thermal/intrusive origin for ductile deformation and probably doming, which has been suggested as a trigger of ductile deformation here of in other MCCs (Lister & Baldwin, 1993; Terrien, 2012). A transient thermal peak related to the Catalina Intrusive Suite may have been able to promote ductile deformation in the shallow crust for a short period, long enough to develop the mylonite fabric. Our data however show that the main ductile and the brittle fabrics of the Catalina MCC developed at different times and while the Catalina forerange was indeed at shallow depths at the time of brittle detachment development.

The earlier Cenozoic tectonic framework driving the magmatic/metamorphic history of the area preceding the 25 Ma doming and extension remains to be resolved. In other words, one needs to resolve what drove the formation of the extensive intracrustal, S-type Wilderness Sills Suite, the ductile fabric (crustal flow of some sort), and the protracted high temperature (all Eocene and possibly into the Oligocene) recorded in the Catalina range. We suspect that the area was part of the upper middle crust of a hot orogenic plateau (the *Arizonaplano* of Chapman et al., 2020) for much of the early and mid-Cenozoic, but more studies are needed for a fuller understanding of the Cenozoic evolution of the Catalina-Rincon Mountains and southern Arizona in general. With regard to the Catalina MCC, its original significance needs to be adjusted since the brittle and main ductile fabrics are demonstrably not synchronous.

Data Availability Statement

All data reported in this study are given in the supporting information tables and were uploaded into the OSF (Open Science Framework) database: New timing and depth constraints for the Catalina Metamorphic Core complex, Southeast Arizona. Retrieved from osf.io/aurzn (Ducea, 2020).

Acknowledgments

M. N. D. acknowledges support from the Romanian Executive Agency for Higher Education, Research, Development and Innovation Funding project PN-III-P4-ID-PCCF-2016-0014. Numerous discussions and field trips with George Davis, George Gehrels, Peter DeCelles, and the late Bill Dickinson have sharpened our view of the Catalina MCC. Former students Steve Kidder, Brendon Johnson, Derek Hoffman, and Lucia Profeta participated in sample collection and/or data acquisition in the early stages of this project. Reviews by John Singleton, J. Lawford Anderson, and Raphaël Gottardi were exceptionally useful in improving an earlier version of this manuscript. We also thank chief editor John Geissmam for guidance.

References

Anderson, J. L., Barth, A. P., Wooden, J. L., & Mazdab, F. (2008). Thermometers and thermobarometers in granitic systems. *Reviews in Mineralogy and Geochemistry*, *69*(1), 121–142.

Anderson, J. L., Barth, A. P., & Young, E. D. (1988). Mid-crustal cretaceous roots of Cordilleran metamorphic core complexes. *Geology*, *16*, 366–369.

Anderson, J. L., & Smith, D. R. (1995). The effects of temperature and oxygen fugacity on the Al in-hornblende barometer. *American Mineralogist*, *80*, 549–559.

Best, M. G., Christiansen, E. H., de Silva, S., & Lipman, P. W. (2016). Slab-rollback ignimbrite flareups in the southern Great Basin and other Cenozoic American arcs: A distinct style of arc volcanism. *Geosphere*, *12*(4), 1097–1135.

Blundy, J. D., & Holland, T. J. B. (1990). Calcic amphibole equilibria and a new amphibole plagioclase geothermometer. *Contributions to Mineralogy and Petrology*, *104*(2), 208–224. https://doi.org/10.1007/BF00306444

Chapman, J. B., Ducea, M. N., DeCelles, P. G., & Profeta, L. (2015). Tracking changes in crustal thickness during orogenic evolution with Sr/Y: An example from the North American Cordillera. *Geology*, *43*(10), 919–922.

Chapman, J. B., Grieg, R., & Haxel, G. B. (2020). Geochemical evidence for an orogenic plateau in the southern U.S. and northern Mexican Cordillera during the Laramide orogeny. *Geology*, *48*(2), 164–168. https://doi.org/10.1130/G47117.1

Coney, P. J., & Harms, T. A. (1984). Cordilleran metamorphic core complexes: Cenozoic extensional relics of Mesozoic compression. *Geology*, *12*, 550–554.

Crittenden, M. D. Jr., Coney, P. J., & Davis, G. H. (1978). Penrose conference report: Tectonic significance of metamorphic core complexes in the North American Cordillera. *Geology*, *6*, 79–80.

Crittenden, M. D. Jr., Coney, P. J., & Davis, G. H. (1980). Cordilleran metamorphic core complexes. *Geological Society of America Memoirs*, *153*, 490. https://doi.org/10.1130/MEM153-p485

Davis, G. H. (1980). Structural characteristic of metamorphic core complexes, southern Arizona. In M. D. Crittenden, Jr., P. J. Coney, & G. H. Davis (Eds.), *Cordilleran metamorphic core complexes*, *Geological Society of America Memoir* (Vol. 153, pp. 35–78). America: Geological Society of America. https://doi.org/10.1130/MEM153-p35

Davis, G. H., & Coney, P. J. (1979). Geologic development of the Cordilleran metamorphic core complexes. *Geology*, *7*, 120–124.

Delph, J. R., Ward, K. M., Zandt, G., Ducea, M. N., & Beck, S. L. (2017). Imaging a magma plumbing system from MASH zone to magma reservoir. *Earth and Planetary Science Letters*, *457*, 313–324. https://doi.org/10.1016/j.epsl.2016.10.008

Dickinson, W. R. (1991). Tectonic setting of faulted tertiary strata associated with the Catalina core complex in southern, Arizona: Geol. Soc. Am. Spec Paper 264.

Dodson, M. H. (1973). Closure temperature in cooling geochronological and petrological systems. *Contributions to Mineralogy and Petrology*, *40*(3), 259–274. https://doi.org/10.1007/BF00373790

Drew, S. T., Ducea, M. N., & Schoenbohm, L. M. (2009). Mafic volcanism on the Puna plateau, NW Argentina: Implications for lithospheric composition and evolution with an emphasis on lithospheric foundering. *Lithosphere*, *1*(5), 305–318.

DuBois, R. L. (1959). Geology of the Santa Catalina Mountains: Arizona Geological Society, Southern Arizona Guidebook II: 107–116.

Ducea, M. (2020). New timing and depth constraints for the Catalina metamorphic Core complex, Southeast Arizona. Retrieved from OSF. IO/aurzn, DOI https://doi.org/10.17605/OSF.IO/AURZN

Ducea, M. N., Ganguly, J., Rosenberg, E. J., Patchett, P. J., Cheng, W., & Isachsen, C. (2003). Sm–Nd dating of spatially controlled domains of garnet single crystals: A new method of high-temperature thermochronology. *Earth and Planetary Science Letters*, *213*(1–2), 31–42. https://doi.org/10.1016/S0012-821X(03)00298-X

Ducea, M. N., & Saleeby, J. B. (1998). The age and origin of a thick mafic–ultramafic keel from beneath the Sierra Nevada batholith. *Contributions to Mineralogy and Petrology*, *133*(1–2), 169–185. https://doi.org/10.1007/s004100050445

Eberlei, T., Habler, G., Wegner, W., Schuster, R., Korner, W., Thoni, M., & Abart, R. (2015). Rb/Sr isotopic and compositional retentivity of muscovite during defromation. *Lithos*, *227*, 161–178. https://doi.org/10.1016/j.lithos.2015.04.007

Erak, D., Matenco, L., Toljić, M., Stojadinović, U., Andriessen, P. A. M., Willingshofer, E., & Ducea, M. N. (2017). From nappe stacking to extensional detachments at the contact between the Carpathians and Dinarides–the Jastrebac Mountains of Central Serbia. *Tectonophysics*, *710*, 162–183.

Fayon, A. K., Peacock, S. M., Stump, E., & Reynolds, S. J. (2000). Fission track analysis of the footwall of the Catalina detachment fault, Arizona: Tectonic denudation, magmatism, and erosion. *Journal of Geophysical Research*, *105*(B5), 11,047–11,062. https://doi.org/10.1029/1999JB900421

Fornash, K. F., Patchett, P. J., Gehrels, G. E., & Spencer, J. E. (2013). Evolution of granitoids in the Catalina metamorphic core complex, southeastern Arizona: U–Pb, Nd, and Hf isotopic constraints. *Contributions to Mineralogy and Petrology*, *165*(6), 1295–1310.

Freeman, S. R., Inger, S., Butler, R. W. H., & Cliff, R. A. (1997). Dating deformation using Rb-Sr in white mica: Greenschist facies deformation ages from the Entrelor shear zone, Italian Alps. *Tectonics*, *16*(1), 57–76. https://doi.org/10.1029/96TC02477

Garzione, C. N., McQuarrie, N., Perez, N. D., Ehlers, T. A., Beck, S. L., Kar, N., et al. (2017). Tectonic evolution of the central Andean plateau and implications for the growth of plateaus. *Annual Review of Earth and Planetary Sciences*, *45*(1), 529–559. https://doi.org/10.1146/annurev-earth-063016-020612

Gehrels, G. E. & Pecha, M. (2014). Detrital zircon U-Pb geochronology and Hf isotope geochemistry of Paleozoic and Triassic passive margin strata of western North America. *Geosphere*, *10*, 49–65.

Gehrels, G.E., Valencia, V., & Pullen, A. (2006). Detrital zircon geochronology by laser-ablation multicollector ICPMS at the Arizona LaserChron center, in T. Loszewski, & W. Huff (Eds.), Geochronology: Emerging opportunities, paleontology Society Short Course. Paleontology Society Papers 11.

Gehrels, G. E., Valencia, V., & Ruiz, J. (2008). Enhanced precision, accuracy, efficiency, and spatial resolution of U-Pb ages by laser ablation–multicollector–inductively coupled plasma–mass spectrometry. *Geochemistry, Geophysics, Geosystems*, *9*, Q03017. https://doi.org/10.1029/2007GC001805

Keith, S. B., Reynolds, S. J., Damon, P. E., Shafiqullah, M., Livingston, D. E., & Pushkar, P. D. (1980). Evidence for multiple intrusion and deformation within the Santa Catalina-Rincon-Tortolita crystalline complex, southeastern Arizona. In M. D. Crittenden, P. J. Coney, & G. H. Davis (Eds.), *Cordilleran metamorphic core complexes*, *Geological Society of America Memoir* (Vol. 153, pp. 217–268). America: Geological Society of America. https://doi.org/10.1130/MEM153-p217

Leake, B. E., Woolley, A. R., Birch, W. D., Burke, E. A., Ferraris, G., Grice, J. D., & Stephenson, N. C. (2004). Nomenclature of amphiboles: Additions and revisions to the international mineralogical Association's amphibole nomenclature. *Mineralogical Magazine*, *68*(1), 209–215. https://doi.org/10.1180/0026461046810182

Lingrey, S. H. (1982). *Structural geology and tectonic evolution of the northeastern Rincon mountains, Cochise and Pima Counties, Arizona, (Doctoral Dissertation)*. Tucson, AZ: University of Arizona.

Lister, G. S., & Baldwin, S. L. (1993). Plutonism and the origin of metamorphic core complexes. *Geology*, *21*(7), 607–610. https://doi.org/10.1130/0091-7613(1993)021<0607:PATOOM>2.3.CO;2

Lister, G. S., & Davis, G. A. (1989). The origin of metamorphic core complexes and detachment faults formed during tertiary continental extension in the northern Colorado River region, U.S.A. *Journal of Structural Geology*, *11*(1–2), 65–94. https://doi.org/10.1016/0191-8141(89)90036-9

Ludwig, K. (2008). Isoplot 3.60: Berkeley geochronology center, Special Publication No 4, 25 pp.

McGrew, A. J., Peters, M. T., & Wright, J. E. (2000). Thermobarometric constraints on the tectonothermal evolution of the East Humboldt range metamorphic core complex, Nevada. *Geological Society of America Bulletin*, *112*, 45–60.

Muller, W. (2003). Strengthening the link between geochronology, textures and petrology. *Earth and Planetary Science Letters*, *206*, 237–251.

Otamendi, J. E., Ducea, M. N., Tibaldi, A. M., Bergantz, G. W., de la Rosa, J. D., & Vujovich, G. I. (2009). Generation of Tonalitic and Dioritic magmas by coupled partial melting of gabbroic and Metasedimentary rocks within the deep crust of the Famatinian magmatic arc, Argentina. *Journal of Petrology*, *50*, 841–873.

Peters, L., Ferguson, C. A., Spencer, J. E., Orr, T. R., & Dickinson, W. R. (2003). *Sixteen $^{40}Ar/^{39}Ar$ geochronology analyses from Southeastern Arizona (OFR-03-02)*. Tucson, AZ: Arizona Geological Survey.

Pullen, A., Ibáñez-Mejia, M., Gehrels, G. E., Giesler, D., & Pecha, M. (2018). Optimization of a laser ablation-single collector-inductively coupled plasma-mass spectrometer (thermo element 2) for accurate, precise, and efficient zircon U-Th-Pb geochronology. *Geochemistry, Geophysics, Geosystems*, *19*, 3689–3705. https://doi.org/10.1029/2018GC007889

Reynolds, S. J. (1985). Geology of the South Mountains, Central Arizona. Arizona Geological Survey Bulletin-195, 75 p., 1 map plate, scale 1:24,000.

Reynolds, S. J., Shafiqullah, M., Damon, P. E., & DeWitt, E. (1986). Early miocene mylonitization and detachment faulting, South Mountains, Central Arizona. *Geology*, *14*(4), 283. https://doi.org/10.1130/0091-7613(1986)14<283:EMMADF>2.0.CO;2

Shakel, D. W., Silver, L. T., & Damon, P. E. (1977). Observations on the history of the gneissic core complex, Santa Catalina Mountains, southern Arizona. *Geological Society of America Abstracts with Programs*, *9*, 1169–1170.

Singleton, J. S., Seymour, N. M., Reynolds, S. J., Vomocil, T., & Wong, M. S. (2019). Distributed Neogene faulting across the western to central Arizona metamorphic core complex belt: Synextensional constriction and superposition of the Pacific-North America plate boundary on the southern Basin and Range. *Geosphere*, *15*, 1409–1435. https://doi.org/10.1130/GES02036.1

Singleton, J. S., Stockli, D. F., Gans, P. B., & Prior, M. G. (2014). Timing, rate, and magnitude of slip on the buckskin-rawhide detachment fault, west-central Arizona. *Tectonics*, *33*, 1596–1615. https://doi.org/10.1002/2013TC003517

Spencer, J. E., & Reynolds, S. J. (1989). Middle tertiary tectonics of Arizona and adjacent areas: Geologic evolution of Arizona. *Arizona Geological Society Digest*, *17*, 539–574.

Spencer, J. E., Richard, S. M., Lingrey, S. H., Johnson, B. J., Johnson, R. A., & Gehrels, G. E. (2019). Reconstruction of mid-Cenozoic extension in the Rincon Mountains area, southeastern Arizona, USA, and geodynamic implications. *Tectonics*, *38*, 2338–2357. https://doi.org/10.1029/2019TC005565

Spencer, J. E., Richard, S. M., Reynolds, S. J., Miller, R. J., Shafiqullah, M., Gilbert, W. G., & Grubensky, M. J. (1995). Spatial and temporal relationships between mid-tertiary magmatism and extension in southwestern Arizona. *Journal of Geophysical Research*, *100*(B6), 10,321–10,351. https://doi.org/10.1029/94JB02817

Terrien, J. (2012). The role of magmatism in the Catalina metamorphic core complex, Arizona: Insights from integrated thermochronology, Gravity and Aeromagnetic Data: Earth Sciences - Dissertations. Syracuse University PhD.

Toljić, M., Matenco, L., Ducea, M. N., Stojadinović, U., Milivojević, J., & Đerić, N. (2013). The evolution of a key segment in the Europe–Adria collision: The Fruška Gora of northern Serbia. *Global and Planetary Change*, *103*, 39–62. https://doi.org/10.1016/j.gloplacha.2012.10.009

Villa, I. M. (2016). Diffusion in mineral geochronometers: Present and absent. *Chemical Geology*, *420*, 1–10.

Ward, K. M., Delph, J. R., Zandt, G., Beck, S. L., & Ducea, M. N. (2017). Magmatic evolution of a Cordilleran flare-up and its role in the creation of silicic crust. *Nature Scientific Reports*, *7*(1), 9047. https://doi.org/10.1038/s41598-017-09015-5

Wernicke, B. (1985). Uniform-sense normal simple shear of the continental lithosphere. *Canasian Journal of Earth Science*, *22*, 108–126.

Wernicke, B. (1992). Cenozoic extensional tectonics of the U.S. Cordillera. In B. C. Burchfiel, P. W. Lipman, & M. L. Zoback (Eds.), *The Cordilleran Orogen; conterminous U.S. the geology of North America* (pp. 553–581). Boulder, Colorado: Geological Society of America.

Whitney, D. L., Teyssier, C., Rey, P., & Buck, W. R. (2013). Continental and oceanic core complexes. *GSA Bulletin*, *125*(3–4), 273–298. https://doi.org/10.1130/B30754.1